JOURNAL OF CATALYSIS 61, 397–411 (1980)

Model Studies on Bimetallic Cu/Ru Catalysts

I. Cu on Ru(0001)

K. CHRISTMANN, G. ERTL, AND H. SHIMIZU[1]

Institut für Physikalische Chemie der Universität München, D-8000 München 2, Sophienstrasse 11, West Germany

Received April 13, 1979; revised July 26, 1979

Thin copper overlayers on a Ru single-crystal surface were prepared as models for Cu/Ru "bimetallic cluster" catalysts. Various amounts of copper were deposited at 540 K on a ruthenium(0001) crystal surface. LEED, AES, thermal desorption (TDS), and work function ($\Delta\varphi$) measurements suggested an overall growth process which may de divided into three stages: (1) An exclusively two-dimensional Cu growth phase (I) exhibits randomly distributed Cu nuclei ranging up to a surface coverage of approximately 8×10^{14} Cu atoms/cm^2 (which corresponds to 50–60% of a Ru monolayer). (2) In region II coalescence and transition from the two-dimensional to the three-dimensional Cu phase occurs. The coverage ranges from $\theta_{Cu} = 0.6$ up to $\theta_{Cu} = 1$–2. (3) Finally, three-dimensional layer growth occurs in stage III leading to an epitaxial Cu film with pronounced (111) orientation. Two thermal desorption states β_1 and β_2 can be directly correlated with the three-dimensional and the two-dimensional growth, respectively. The activation energies for desorption are about 80 kcal/mole for the β_1 and 84 kcal/mole for the β_2 state. The work function of the clean Ru(0001) surface ($\varphi_{Ru} = 4.5$ eV) increases upon Cu deposition by 0.70 eV during stage I, exhibits a flat intermediate maximum in the transition stage, and decreases finally to the value of the Cu(111) face ($\varphi_{Cu} = 4.9$ eV). The (slight) electron transfer from Ru to Cu is interpreted in terms of an almost covalent chemisorption bond and is evidence of an electronic interaction between the two metals.

1. INTRODUCTION

The catalytic activity and selectivity of a metal may often be strongly affected by alloying with a second component, and numerous fundamental studies in this field have been performed in the past (*1, 2*). In recent years a new class of bimetallic catalysts has been developed which consists of very small particles of metallic combinations which do not form bulk alloys and for which the term "bimetallic clusters" was proposed (*2, 3*). Systems of this type are for example the basis of an effective reforming catalyst (*4, 5*). The combination Ru/Cu is an example of this class, for which it was concluded on the basis of indirect information that the copper atoms might tend to cover the surface of ruthenium (*6*). Electron microscopic studies showed that Ru/Cu clusters are very thin and consist possibly of a layer of Ru atoms covered by Cu atoms (*7*). This view was supported by the results of XPS investigations (*8*) which in addition revealed no evidence for an appreciable charge transfer between the constituents connected with detectable shifts of core level binding energies.

These findings impelled us to start an extended series of experiments with well-defined single-crystal surfaces modeling the Cu/Ru "bimetallic clusters" in order to obtain a better microscopic understanding of the processes occuring at the surfaces of these interesting systems. Following Sinfelt's conclusions on the structure, our model system consists of a clean Ru(0001) surface onto which various amounts of Cu were evaporated. The present paper deals with the structural, energetic, and electronic characterization of these systems, and it will be shown among others that Cu atoms indeed tend to form a monoatomic

[1] Permanent address: Electrotechnical Laboratory, Tanashi, Tokyo, Japan.

0021-9517/80/020397-15$02.00/0

overlayer on the Ru surface before three-dimensional crystal growth occurs. A succeeding paper contains the results of studies on the adsorption of hydrogen where close analogies with the findings with "real" Cu/Ru catalysts (*6*) were obtained which justifies the present single-crystal systems as proper models for the bimetallic cluster catalysts. A brief compilation of the results on the growth of thin Cu films on Ru(0001) has been published recently elsewhere (*9*).

2. EXPERIMENTAL

The experiments were performed in a 120 l stainless-teel system (Varian) with a base pressure of approximately 10^{-8} Pa. The apparatus contained facilities for low-energy electron diffraction (LEED), a cylindrical mirror analyser for Auger electron spectroscopy (AES), a quadrupole mass filter for thermal desorption studies, and a Kelvin vibrating capacitor electrode for work function measurements. Futhermore, an electronically regulated Cu evaporation source was attached to the system, details of which have been described elsewhere (*10*). The Ru(0001) sample was prepared by cutting a cylindrical slice from a Ru bulk single crystal with 99.999% purity (diameter ~0.5 cm) and was properly oriented by X-ray techniques. The front face was mechanically polished and carefully precleaned with acetone and distilled water. No chemical etching was performed in order to prevent surface contamination. The crystal was mounted between two tungsten wires and fixed to the sample manipulator. The temperature of the sample could be measured with a chromel–alumel thermocouple spotwelded onto the rear of the crystal. A programmable dc power supply (*11*) served for heating up to 1500 K, whereas cooling down to 150 K was achieved by a commercial liquid N_2 cooling coil device (Varian). The copper used for evaporation was precleaned by melting it in a hydrogen atmosphere onto a tungsten spiral which was mounted inside the deposition device. High-purity hydrogen could be admitted to the system via a bakeable leak valve (Varian). The total gas pressure could be measured with an ionization gauge (Bayard–Alpert type) which also served for a calibration of the mass spectrometer. The pressure data were corrected with respect to hydrogen by the manufacturer's gauge conversion factor. The Ru sample was first cleaned by heating it in oxygen at 1300 K for several minutes. The main contaminant was carbon, the AES signal of which is unfortunately completely masked by a strong Ru Auger transition at 281 eV. It was therefore assumed that the carbon peak height contributes linearly to the Ru 281 eV peak intensity. During the experiments it was found that a ratio of 0.80 between the positive and negative Ru 281 eV signal (the first deviation of N(E) was monitored) corresponds to a clean surface, whereas smaller values strongly suggest the presence of carbon contaminations.

In the course of the experiments it became evident that effective cleaning was obtained by repeated mild Ar^+ ion bombardment and subsequent annealing cycles and by an oxidation/reduction treatment, although admission of oxygen to the belljar always led to an increase of the CO background level. The formation of carbon due to CO dissociation on the sample could be minimized by keeping the AES electron excitation beam current below 1 μA. The LEED pattern of the clean Ru(0001) surface exhibited sharp and bright diffraction spots with a very low background intensity. Small amounts of C gave rise to a formation of a complex LEED pattern similar to that observed previously by Grant and Haas (*12*). Adsorption of carbon monoxide or oxygen led to the same LEED features which were reported in detail by Menzel and co-workers (*13–15*). In addition to LEED and AES, the most sensitive monitor of the state of surface cleanliness was the reproducibility of the hydrogen-induced work function change, as has already been ob-

served with other hydrogen chemisorption systems, e.g., with Ni(111)/H (*16, 17*) or Pt(111)/H (*18*). In the case of Ru(0001) even very low C concentrations (below the detection limit of any other method) give rise to a dramatic change of the $\Delta\varphi$-exposure relation, a point which has been scrutinized by Menzel and Feulner (*19*).

The evaporated copper films were always very clean and did not even show carbon or sulfur impurities, provided that the evaporation source had been outgassed at 1000 K for several hours prior to deposition. The success of this cleaning procedure could be nicely followed by a measurement of the thermal electron emission current which, after some fluctuations, became stable after approximately 2 or 3 hr.

A copper deposition experiment was performed as follows: After the source emission current had become stable, a constant emission of, say, 333 nA was adjusted, and the sample was exposed to the Cu flux for various periods of time. After each deposition the condensed Cu atoms were completely thermally desorbed and monitored with the mass spectrometer. A typical calibration curve is reproduced in Fig. 1 which clearly shows the fairly good linearity between the deposited amount of Cu and the exposure time. Note, however, that the condensation coefficient of Cu, κ_{Cu}, changes when a Cu atom from the vapor phase strikes an adsorbed Cu atom instead of a Ru atom: This leads to an increase of the slope of the straight line of Fig. 1, thus indicating that Cu concentration, above which further deposition leads to more or less exclusive growth in the third dimension. Calibration of the absolute Cu concentrations was achieved by combination with the AES results as will be discussed below.

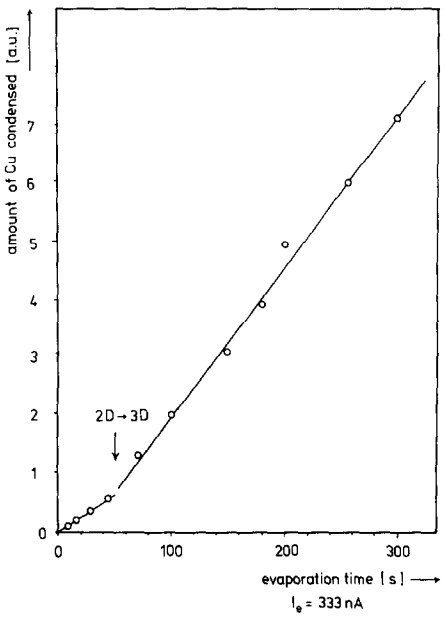

FIG. 1. Amount of copper deposit as determined by TDS (in arbitrary units) as a function of the exposure time (sec). A constant Cu flux of approximately 1×10^{14} cm^2 sec^{-1} ($\pm 50\%$) was chosen during the experiment (corresponding to an electron emission current of the Cu source of 0.33 μA). The sample temperature was 539 K.

3. RESULTS

One of the main purposes of this part of our work was the development of a reproducible technique to prepare well-defined Cu overlayers on a Ru surface as far as the structure and the surface concentration are concerned. Only those surfaces were considered to be suitable for subsequent gas adsorption experiments. Experiments at substrate temperatures between 290 and 700 K showed only little temperature effect on the structural order of the deposit; in general a temperature of 540 K was chosen during Cu evaporation. This fairly high sample temperature renders the impinging Cu atoms sufficiently mobile to reach the binding sites with the lowest free energy. Temperatures above 800 K, however, lead to a marked decrease of the amount of Cu condensed per unit time because desorption becomes now a competitive process.

3.1. LEED

The progress of the Cu deposition process can be directly followed by inspection of the LEED pattern. Starting off with the clean Ru(0001) surface (the LEED pat-

tern of which shows bright and sharp diffraction spots) a marked increase of the background intensity is observed after the deposition of ca. 1.5×10^{13} Cu atoms/cm^2 (for calibration see Section 3.2). This suggests that Cu nuclei are randomly distributed over the ruthenium surface, or very small ordered Cu aggregates are present whose size is far below the coherence width of the electron beam. It cannot be decided whether at this stage the nuclei consist of single Cu atoms or of oligomers. Therefore only little can be said about the size of the critical embryo which governs the stability of the growth. Annealing up to 800 K does not cause any ordering phenomena, and it is thus suggested that the random Cu distribution represents the equilibrium configuration at this stage of the growth process. After further deposition to approximately $2–5 \times 10^{14}$ Cu atoms/cm^2 coalescence of the nuclei occurs, and new diffraction features arise which are shown in Fig. 2a: Double scattering processes of the elec-

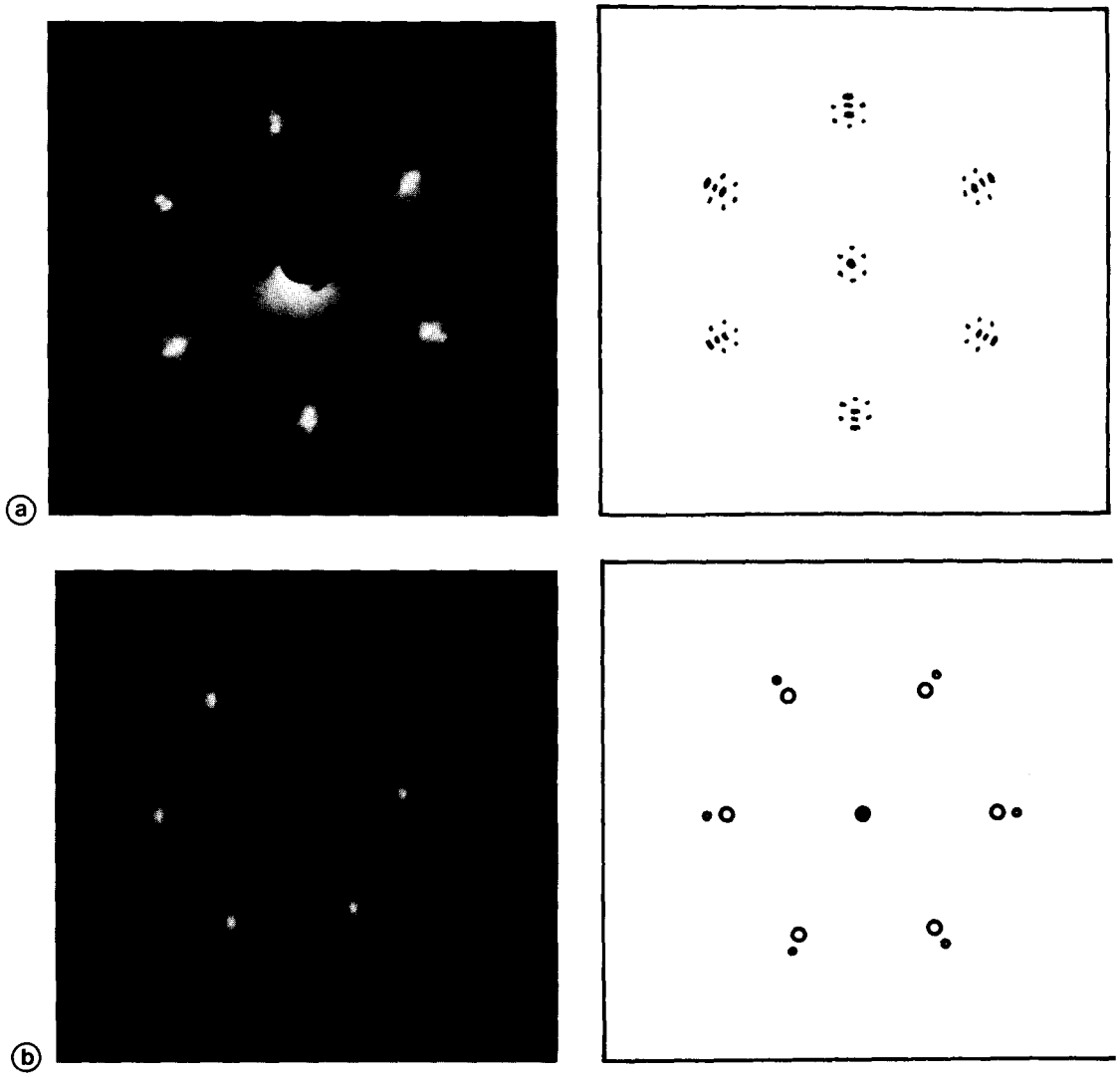

FIG. 2. LEED patterns (electron energy 63 eV). (a) Multiple scattering satellite structure produced by a Cu deposit of approximately $2–5 \times 10^{14}$ Cu atoms/cm^2 on top of the Ru(0001) surface at $T = 539$ K. (b) Superposition of diffraction spots from Ru (inner spots) and from Cu (outer spots), corresponding to a Cu surface concentration of approximately $1–4 \times 10^{15}$ atoms/cm^2.

trons between the topmost Ru atoms and the adjacent Cu atoms give rise to satellites around the diffraction spots due to the Cu overlayer which exhibits a preferred (111) orientation. The quite distinct multiple scattering features indicate a marked two-dimensional growth and react fairly sensitive to the evaporation conditions: They are, for example, much less pronounced if the deposition is performed at temperatures lower than 500 K.

Upon further addition of Cu (to concentrations of approximately 1–4 $\times$ 10^{15} Cu atoms/cm^2) a distinct three-dimensional epitaxial Cu overlayer is built up as can be seen from Fig. 2b. The LEED pattern now consists of a superposition of the two hexagonal spot systems from both the Cu and the Ru lattices, according to the epitaxial relationships: (111) Cu‖(0001) Ru and [101] Cu‖[1010] Ru. Taking the Ru lattice constant $a_{0,\mathrm{Ru}}$ = 2.695 Å as a reference the lattice parameter for the Cu overlayer, $a_{0,\mathrm{Cu}}$, can be directly derived from the geometry of the LEED pattern and is found to be approximately 3.60 Å, which value agrees well with that of bulk copper. Further continuation of the Cu deposition causes a gradual decrease of the diffraction contribution from the Ru lattice. The disappearance of the multiple scattering spots is followed by the disappearance of the LEED features due to ruthenium, leaving only those arising from the Cu lattice. From Auger electron spectroscopy (cf. Section 3.2), where the Ru signal intensity is suppressed at this stage of growth, too, a thickness of approximately 8–10 Cu layers at this stage is derived.

3.2. *Auger Electron Spectroscopy*

It is well established that under certain experimental conditions (*20*) the Auger signal intensity, i.e., the peak-to-peak amplitude of the second derivative of the measured electron current, is proportional to the number of excitation/deexcitation processes and therefore does reflect the actual number of atoms being present in the surface region. Thus, by using the AES signal of the clean metals Cu and Ru (measured under identical experimental conditions) as a standard the relative surface concentrations of these two elements can be determined. All AES data refer to the $CuM_{2,3}M_4M_4$ transition at 62 eV and to the $RuM_5N_{4,5}N_{4,5}$ transition at 281 eV and yield mainly information about the topmost surface region according to the universal mean-free-path-energy relation of metallic solids (*21*). Figure 3 shows the increase of the Cu 62 eV AES signal and the decrease of the Ru 281 eV signal as a function of evaporation time with the deposition rate being kept constant. A more informative diagram might be Fig. 4 where the ratio y between the signal heights of Cu and Ru is plotted against the total condensed amount of Cu as determined by separate thermal desorption experiments (cf. Section 3.3). The data points have been obtained at various deposition times at a constant flux of Cu atoms (approximately 1 $\times$ 10^{14} cm^{-2} sec^{-1}). It is evident from Fig. 4 that an

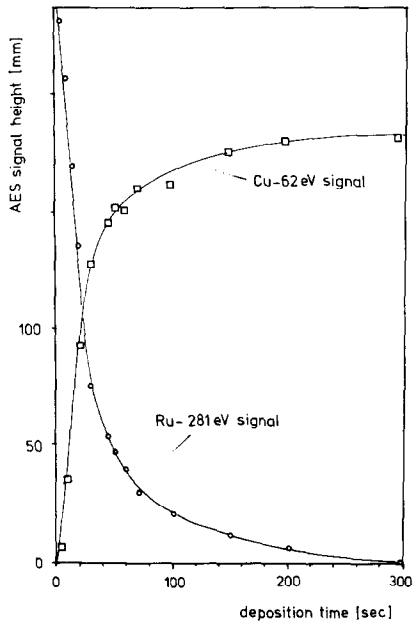

FIG. 3. Variation of the Ru 281 eV AES signal and of the Cu 62 eV AES signal as a function of the Cu deposition time. The Cu flux and the sample temperature were the same as in Fig. 1.

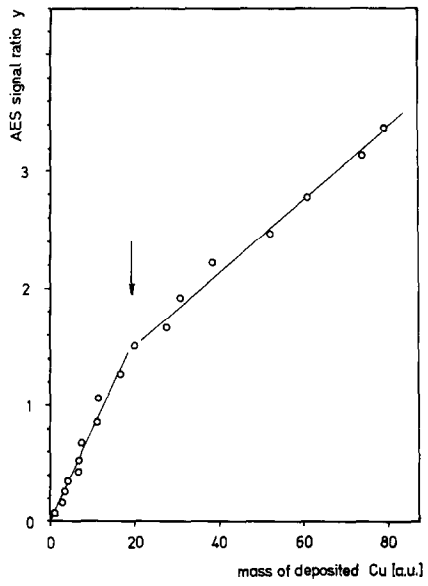

FIG. 4. Plot of the Auger signal ratio y = (Cu 62 eV/Ru 281 eV) versus the overall deposited amount of Cu (determined by TDS). The arrow indicates the transition 2 D → 3 D.

initial linear increase of the signal ratio is followed by a distinct break at approximately 20–25 sec evaporation time (corresponding to a ratio $y = 1.5$) which indicates the onset of the three-dimensional Cu growth. Finally, after approximately 300 sec, the Ru AES signal disappears completely. The corresponding Cu thermal desorption spectrum therefore reflects just that Cu concentration or Cu overlayer thickness which suppresses the Auger electrons excited from Ru atoms below the limits of detection (<5% of a monolayer). The actual thickness of this layer (if uniform distribution of the Cu atoms is assumed) is estimated from the mean free path of electrons, λ, with a kinetic energy of 281 eV (Ru AES signal) in copper. According to various data from the literature (*21–23*) a value of $\lambda = 7$ Å is taken. If an exponential decrease of the Auger signal with penetrated layer thickness is assumed (*24*) it appears that a Cu concentration of roughly 6×10^{15} atoms/cm^2 will damp the Ru 281 eV AES-signal to about $1/e = 37\%$ of its initial intensity. This number corresponds to approximately three atomic layers with (111)-orientation. This value was used for calibrating the absolute Cu concentration on the surface. Unfortunately it is rather crude and certainly not accurate to more than about 30%.

3.3 Thermal Desorption Spectroscopy (TDS)

Figures 5a–c show three series of thermal desorption spectra of Cu from Ru(0001) obtained with a linear heating rate of 10 K/sec. The three sets correspond to different recorder sensitivities with respect to the desorption rate. The enlarged scale of Fig. 5a shows the initial stage of the Cu growth process. Evidently, the very first Cu atoms chemisorbed on the Ru surface are held in a binding state denoted as β_2, the desorption kinetics apparently being close to a 0th order. This state reflects Cu coverages up to approximately 5×10^{14} atoms/cm^2 and can be ascribed to the two-dimensional growth whose termination can be correlated with the completion of the β_2 desorption state. The saturated β_2 state exhibits a maximum desorption temperature of 1220 K (±2%). Higher Cu exposures cause the appearance of a second binding state, β_1, at temperatures below that of the β_2 state. Within a short period of Cu deposition both states grow simultaneously as can be seen from Fig. 5b, but upon further addition of Cu an exclusive increase of the β_1 state is observed which is identified with the three-dimensional growth of copper. The kinetics of the desorption process of the β_1 state also reveals a zeroth-order, indicating that the rate of desorption is independent of the Cu concentration on the surface.

The area below a thermal desorption trace is proportional to the surface concentration of the desorbing species. Although the absolute sensitivity of the mass spectrometer for the registration of the Cu mass (63 amu) is not known and thus the desorption rate can be given only on a relative

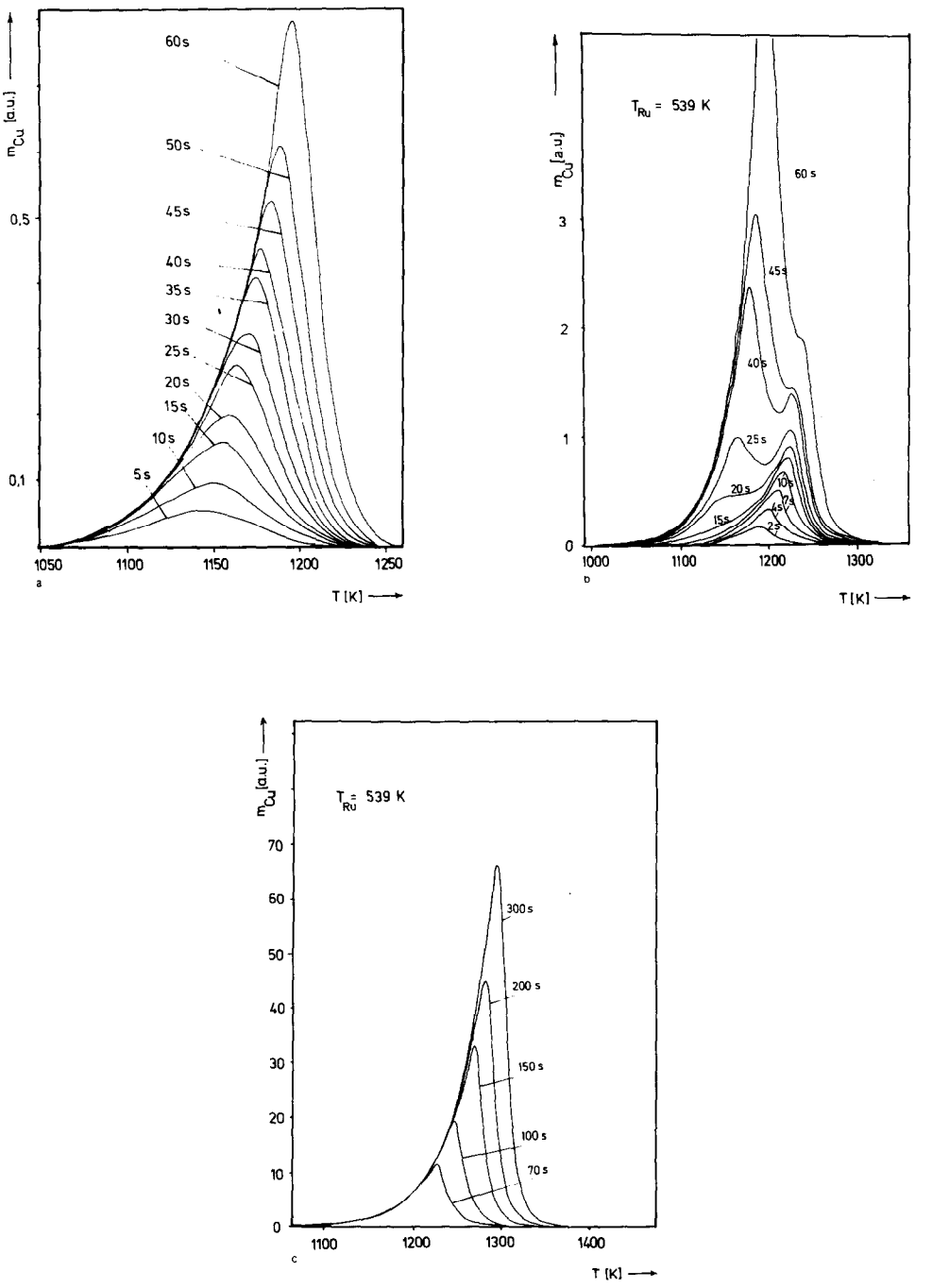

FIG. 5. Thermal desorption spectra of Cu (63 amu) from a ruthenium(0001) surface. The parameter of the curves is the exposure time (at a constant Cu flux). (a) High recorder sensitivity, exposure times ranging from 2 to 60 sec, electron emission current of the source = 0.10 μA, deposition temperature 539 K. Only the β_2 state can be seen in the spectrum. (b) Medium recorder sensitivity, exposure times ranging from 2 to 60 sec, electron emission current of the Cu source now 0.33 μA, sample temperature 539 K. Mainly the β_1 state can be seen in the spectrum, the β_2 state appears only for low exposures. (c) Low recorder sensitivity, exposure times ranging from 70 to 300 sec, deposition rate corresponding to an electron emission current of 0.33 μA.

scale, combination with the AES results (cf. Section 3.2) allows an absolute calibration of the desorbing amounts. Thus, calibration of *relative* Cu surface concentrations from an evaluation of the TDS peak areas is very accurate and free of any further assumptions, whereas *absolute* values are uncertain within the limits of the AES calibration.

If the desorption traces of Fig. 5 are subjected to a lineshape analysis according to King (*25*), the activation energy for the desorption process from both Cu binding states may be derived. The corresponding Arrhenius plots belonging to the β_1 and the β_2 state (each of them containing data points taken at different initial coverages) are shown in Figs. 6a and b. For the β_2 state a desorption energy of the Cu chemisorbed on the Ru surface of approximately 84 (±2) kcal/mole = 351 kJ/mole is obtained which depends only slightly on coverage. From the slope of the straight line shown in Fig. 6b an activation energy of 80 (±2) kcal/mole = 334 kJ/mole irrespective of the coverage is evaluated, which number is in very close agreement with the heat of sublimation of pure bulk copper (*26*). The data evaluation procedure given by King allows also a determination of the reaction order and yields in the case of the β_1 state as well as for the β_2 state (within the limits of accuracy) a desorption order of zero. This quite interesting result will be discussed further in Section 4.

3.4. Work Function Variation

A distinct work function change $\Delta\varphi$ takes place if a clean Ru sample is covered with copper. Figure 7a presents a semilogarithmic plot of $\Delta\varphi$ as a function of Cu deposition. From literature data (*27*) the work function of the clean and well-annealed Ru(0001) surface is taken to be approximately 4.5 eV. The nucleation of Cu and the onset of the coalescence stage leads to an almost linear increase of the work function of the system (shown in Fig. 7b) until a value of approximately 5.2 eV (i.e., $\Delta\varphi$ = 0.7 eV) is reached. A comparison with the corresponding thermal desorption spectra shows that at this stage the two-dimensional growth is nearly completed. However, it has to be kept in mind that under the present conditions no complete copper monolayer was formed prior to the onset of three-dimensional growth. It is highly probable that a uniform Cu monolayer would lead to an even higher value of the work function change. Further addition of copper during this stage causes the onset

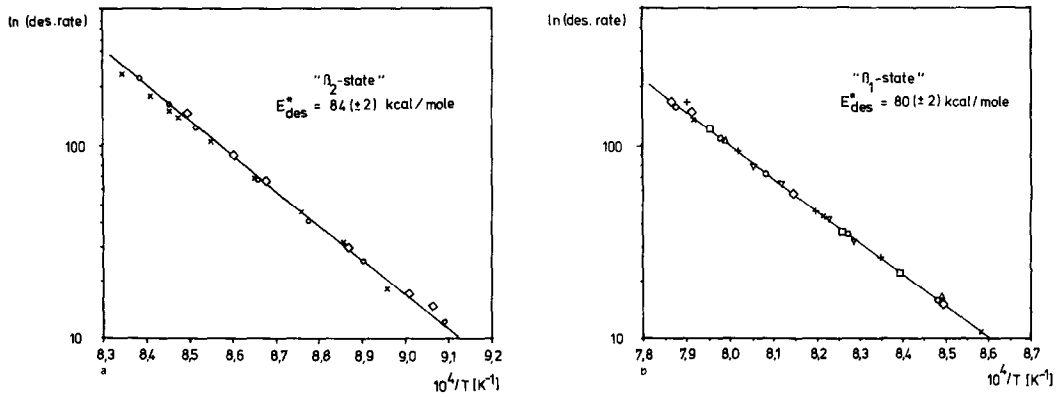

FIG. 6. Arrhenius plots (ln (desorption rate) versus the inverse temperature) of the desorption traces given in Figs. 5a and c, based on a lineshape analysis according to King (*25*). (a) Analysis of the β_2 state. The different symbols indicate different surface Cu coverages. (b) Analysis of the β_1 state for different Cu surface concentrations.

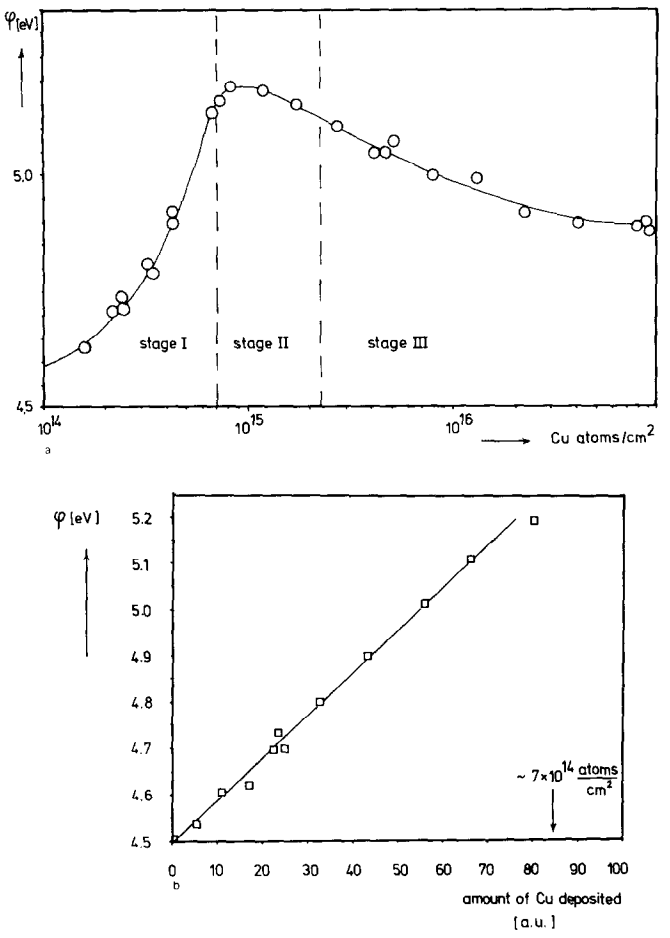

FIG. 7(a) Plot of the Cu induced work function change versus the logarithm of the amount of Cu deposited. The three different Cu growth stages are indicated in the figure. (b) Initial portion of the work function change due to copper versus the total amount of deposit. Note the almost linear increase in this range!

of three-dimensional growth together with completion of the first monolayer and leads to a continuous decrease of φ until finally the work function characteristic for the clean Cu(111) surface is reached. The resulting value is in good agreement with literature data (≈4.9 eV) (*28*). The occurrence of the φ-maximum indicates a slight electronic charge transfer between the Ru surface and the chemisorbed Cu atoms within the first layer. The dipole moment of this chemisorption complex turns out to be fairly small and is estimated to be approximately 0.1. Debye using simple electrostatic arguments (*29*).

4. DISCUSSION

The growth of Cu on the Ru(0001) surface can be regarded mainly under two aspects: First, there is a more macroscopic point of view which utilizes thermodynamics and kinetic theories to describe the individual growth stages and their dependence on the temperature and the deposition rate. This is most commonly used when the phenomenon "epitaxy" is described, and a large number of theories concerning nucleation and coalescence have been developed in the past (*30*). In principle, these theories are capable of pre-

dicting the structure of the Cu films on the Ru surface provided that certain thermodynamic quantities are known (e.g., the surface free energies of Cu and Ru, the activation energy for Cu diffusion, the lattice energies of Cu and Ru, the diffusion constants and their temperature dependence etc.). However, only very poor data exist for the present system, and one can, at the moment, only speculate on the most probable manner of the growth. The present measurements are supporting a three-stage process as will be discussed below.

The second approach consists in a rigorous quantum-mechanical treatment which regards the copper atoms as being chemisorbed on the Ru surface and which can be set up in a somewhat similar manner as the current theories on chemisorption of gases on metals. Several attempts in the literature are concerned mainly with the adsorption of alkali metals on group VIIIb metals (*31*) or the adsorption of noble metals (Ag, Cu) on tungsten (*32*). These theories typically start off with a modified Anderson formalism (which was first introduced into chemisorption theory by Newns (*33*) for the Ni/H system) and consider coupling between electronic states of the adatom and those of the substrate metal. Semiempirical theories utilize the work function of the clean substrate, the ionization potentials, as well as the electron affinity of the adatom as variables. The relative position of the adatom resonance level with respect to the Fermi level of the substrate metal accounts for the degree and direction of the electron transfer, whereas the broadening of the adatom level is mainly determined by the degree of overlap and thus depends on the interatomic distance. The adsorption of Cu on tungsten has been successfully treated in that way by Jones and Roberts (*34*). Like Cu–W, the Cu–Ru system represents a very suitable example for a theoretical description, since there is no evidence for diffusion of Cu into the Ru bulk, nor is there any alloy formation. The chemisorption picture described above can be very helpful in understanding the electronic interaction between Cu and Ru (which governs the experimentally observed work function change to some extent) and may also allow us to estimate the strength of the Cu–Ru bond. It may then be adequate for a description of the very first stages of the Cu growth (i.e., as long as no direct adatom interactions come into play).

The proposed three-stage process for the growth of Cu on Ru simply consists of the exclusive two-dimensional stage (I), a transition region (II) where 2 D and 3 D Cu aggregates exist on the Ru surface, and the three-dimensional epitaxial layer growth of copper (III). These stages can be clearly discerned from our experiments. Concerning stage I, it follows from the LEED observations that no ordered Cu structure is formed in the submonolayer range (which is for example in contrast to alkali metal adsorption on VIIIb metals). This suggests that the Ru(0001) surface has a smooth potential energy surface and that there exist no strong long-range interaction forces between the Cu atoms. However, short-range interactions between adjacent Cu atoms cannot be excluded, since the mean size of small aggregates ($\sim$5 atoms) would be far below the coherence width of the LEED electron beam.

The derived zero-order kinetics for desorption from the Cu β_2 state, on the other hand, could eventually be understood, if one assumes desorption of single Cu atoms from aggregates containing many Cu atoms caused by strong attractive interactions between nearest neighbors. Since it seems rather unlikely that even at very low Cu surface coverages large islands are formed, an alternate explanation is preferred whereafter desorption occurs mainly from a fixed number of favorable sites (presumably structural defects) on the surface. The concentration of these sites does not seem to depend on the surface temperature or the Cu concentration. Strong support for the idea that pairs, triplets, or quadruplets of Cu stick together even during diffusion over

the surface is obtained from field emission investigations on the W/W system by Ehrlich and co-workers (*35*). These studies clearly showed that a correlated diffusion of pairs of W atoms on a W field emission tip is less activated than the diffusion of a single W atom. Detailed investigations by Harsdorff *et al.* (*36*) concerning the initial growth of Au on alkali halide surfaces also give clear evidence for the formation of Au dimers on the surface which do not dissociate under diffusion conditions. For the present Cu–Ru system it is thus concluded that, during the nucleation phase, small clusters of Cu atoms (containing perhaps up to about five to seven atoms) are formed which are randomly distributed over the surface and which are stable even under diffusion conditions (at elevated temperatures). Although no direct information is available from the present study on the diffusion of Cu atoms on a Ru surface, one can try to elaborate some analogies with the similar, but much better investigated Cu–W system. Field emission studies allowed a direct observation of the Cu diffusion boundary line (*37*) or, by utilizing the probe-hole technique, enabled a more quantitative evaluation of diffusion data (*34*). Melmed (*37*) investigated single, double, and triple-layer diffusion of Cu on different crystal planes of tungsten and reported on values for the diffusion activation energies, E_{diff}, and for the diffusion preexponentials, D_0. For a single layer of Cu on a W(110) plane (which is assumed to be as smooth as the hcp(0001) surface) and for a comparable temperature range (300–400°C) he obtained $E_{diff} = 8$ kcal/mole = 0.35 eV, and for D_0 a value of approximately 7×10^{-7} cm^2 sec^{-1}, whereas for the rougher (100) surface appreciably higher numbers were obtained. If the fairly low E_{diff} value for the Cu diffusion on a densely packed smooth metal surface is transferred to the Cu–Ru system (some justification arises from the fairly similar binding energies of the Cu–W(110)- and the Cu–Ru(0001) bond (*37*)) it is likewise to be expected that a high mobility exists within the first single Cu layers on the Ru surface at the temperatures employed during the deposition process. The preferential spreading of Cu atoms on the Ru surface and the formation of a chemisorbed monoatomic overlayer prior to the onset of three-dimensional crystal growth is obviously caused by energetic reasons: The activation energy for Cu desorption from the β_2 state (which is identified with the 2 D Cu) is obviously equal to the binding energy for a Cu atom bound to the Ru surface, it turns out to be approximately 84 kcal/mole = 3.64 eV, which value is slightly higher than that of a Cu atom bound to bulk copper (which should be equal to the heat of sublimation of Cu) as it was obtained from the β_1-TD state to be 80 kcal/mole = 3.51 eV. It is interesting to note that the desorption energy of Cu from a tungsten emitter is very similar, namely 88 kcal/mole = 3.82 eV (*37*). This means that, regardless of the lattice energy of the substrate metal ($E_{latt,Ru}$ = 160 kcal/mole, $E_{latt,W}$ = 202 kcal/mole (*38*)), the Cu atoms are bound to the substrate metal in a fairly similar manner. No satisfactory answer can be offered to the question why not a complete Cu monolayer is formed at 539 K (as follows from the TD spectra), but instead the partial build-up of a second layer begins. Energetic and/or kinetic reasons may account for the early onset of the three-dimensional growth. One could imagine that the formation of a complete single Cu layer needs somewhat higher temperatures than that employed in our deposition experiment, an idea which is supported by the observation that after flashing off just the β_1 state and cooling down again pronounced multiple scattering features in the LEED pattern (cf., Fig. 2a) occur which are characteristic for a well-ordered homogeneous two-dimensional overlayer.

The second stage (II) comprises the transition from the 2 D to the 3 D growth. The plot of the AES Cu–Ru signal ratio versus the amount of deposited Cu (Fig. 4) exhibits

only *one* break. For the Cu/W(110) system Bauer *et al.* (*39*) observed two such breaks in a similar plot which were attributed to a completion of subsequent copper monolayers, and thus the individual build-up of three monolayers could be discerned. In addition, the corresponding TD spectra exhibited two well-separated states which were filled exactly sequentially, opposite to the present TD results for the Cu–Ru system, where in the transition region, a more or less simultaneous growth of the β_1 and the β_2 state appeared. This difference probably arises from the fact that the difference in energy between the two states is considerably lower for Cu/Ru than for Cu/W (*39*), thereby allowing a Cu atom to stick on top of a Cu aggregate, although there are still Ru sites available. Keeping this in mind, an important difference between both systems under consideration emerges: Whereas for Cu–W the continuous growth of individual and complete Cu monolayers is observed (in a manner which has been described by Gomer (*40*) as "unrolling a carpet") there is strong indication for the Cu–Ru system (at least under the present preparation conditions) that complete Cu monolayers are not formed until the coalescence stage facilitates diffusion of Cu on Cu thereby leading to a levelling of the hillock-like surface structure. This concept is supported by the results of the work function measurements (cf. Fig. 7a) which indicate a pronounced maximum at this intermediate range, but (important to note) exhibit only a very gradual decay until the φ value of the Cu(111) surface after the deposition of four or five layers is reached. It will be discussed below, whether the surface roughness or a proper consideration of the charge transfer processes can explain the observed work function features.

The exclusive three-dimensional growth of the Cu deposit (stage III) is indicated by the β_1-TD state, by AES and by LEED. In addition, the latter data clearly demonstrate the epitaxial nature of the deposit. Apart from the multiple scattering pattern (which is assumed to be correlated with the transition stage (II)), there is no evidence for any strain features within the deposit layer, although from the crystallography a misfit in the lattice spacings between Ru (nearest-neighbor distance in the (0001) plane d = 2.695 Å) and Cu ($d(111)$ = 2.551 Å) of about 5% exists. Evidence for any lattice contraction or expansion in the vertical distance could, however, be obtained only from a careful analysis of the LEED intensities which was not performed in the present case.

Work function effects are usually difficult to interprete, since both electronic and geometric factors contribute to this quantity. Whereas so far no data material exists for the Cu–Ru system, again quite extensive work function results are reported for the Cu–W system. As pointed out in Section 3.4, the initial deposition of Cu on the Ru(0001) surface leads to a continuous increase of φ by up to 700 meV. For Cu condensation on W(110) Bauer *et al.* (39) observed effects which depended slightly on the deposition temperature: Room temperature deposition as well as deposition at 800 K cause an initial decrease of φ by about 800 meV until the first two monolayers are completed. A shallow increase follows, the magnitude of which depends on the temperature. It should be emphasized in this context that the crystallographic orientation of the W substrate governs the shape of the $\varphi(\theta_{Cu})$ curve to a large extent, and also influences the thermal desorption features (i.e., the number of states). Here the important role of the binding site geometry becomes quite evident. Following Bauer *et al.* (*39*) in interpreting the work function features and transferring their arguments to the present Cu–Ru system, a variety of reasons can be made responsible for the experimentally observed work function phenomena: One could start off with simple electrostatic dipole considerations, or could argue on the basis of surface roughness according to the concepts of Smoluchowski (*41*). The latter argument suggests

that atoms adsorbed on a smooth surface may cause an increase of the effective atomic roughness (provided that the adatoms are located in a level above the outermost substrate layer and do not penetrate into the lattice). The enhanced roughness then should give rise to a decrease of the average work function of the system. This concept seems to describe the Cu/W(110) system quite well, where an initial decrease of φ is observed, but fails completely in the case of the Cu–Ru system: Although one should likewise expect an increase of the surface roughness of the Ru(0001) surface owing to the formation of small Cu ensembles, no decrease of the work function is found. By using a simple picture which takes into account that the condensing Cu atoms cover the Ru surface the observed work function increase may be described by a superposition of contributions from both Ru(0001) and Cu(111) patches, since the applied Kelvin method measures an average work function of the surface. The occurrence of the work function maximum, however, cannot be explained in this way. As a matter of fact, we are left with a net charge transfer from the Ru surface to the Cu atoms leading to a dipole moment of approximately 0.1D. The net charge transfer causing this effect is only of the order of a few percent of e_0 and would not give rise to appreciable shifts of the core level binding energies which is agreement with the XPS data (*7*), but indicate nevertheless an electronic interaction which might cause the occurrence of a "ligand effect" (*42*) in chemisorption of gases on such Cu/Ru surfaces.

In contrast to adsorption of alkali metals where an appreciable charge transfer causes the occurrence of ionic forces, in the present case a mainly covalent bond with very little charge transfer is formed. Based on considerations by Newns (*33*), Engel and Gomer (*43*) proposed a fairly plausible model for oxygen chemisorption on tungsten, which was also applied to the Cu/W system by Jones and Roberts (*34*): The substrate metal induces a resonance level in the Cu adatom which is capable of forming a chemical bond with electronic states from the Fermi level of the metal. The vacant Cu resonance level can be positioned approximately halfway between the electron affinity level of the free Cu atom (2.4 eV below E_{vac}) and the Cu ionization potential (7.7 eV below E_{vac}) leading to a resonance level at approximately 5 eV below E_{vac}. This level, however, is fairly broad due to the interaction with the substrate metal valence band. The direction of the electron transfer now depends on the position of the Fermi level of the substrate metal which in the case of Ru(0001) is supposed to be approximately 4.5 eV below E_{vac}. From this picture it is evident for the present case that a net charge transfer from the Ru Fermi level to the lower lying Cu resonance level will occur which would be responsible for the observed dipole moment of the adlayer. Of course, this process dominates only as long as only isolated Cu atoms interact with the Ru surface. With increasing Cu coverage the influence of the dipole moment of the very first (and chemisorbed) layer decreases, until finally the build-up of the epitaxial three-dimensional copper deposit exhibits a work function specific for the Cu(111) surface.

After this discussion of the structural and electronic properties of the Cu/Ru(0001) system we return to the starting point of the present series of studies and to the question whether the single-crystalline bimetallic Cu/Ru system may be used as a proper model for "bimetallic" Cu/Ru catalysts. As already mentioned Prestridge *et al.* (*7*) have recently reported on an electron microscopy study of small catalyst particles consisting of Cu–Ru clusters supported on silica. Interestingly, they found fairly large Ru particles with diameters of ~60 Å, which were however very thin ("raft-like"). It was suggested that these particles are built up in a way that layers of Ru atoms are covered by monoatomic Cu layers, i.e., a typical two-dimensional arrangement.

This structure resembles closely the findings of the present work. The reduction procedure used by Sinfelt *et al.* (*6*) in order to form catalysts by precipitation on the silica support consisted in heating the samples at about 500°C for 3 hr, that is 250 degrees higher than the deposition and annealing temperature used throughout the present experiments. Owing to the higher preparation temperature, Sinfelt's catalysts may well exhibit an even more pronounced two-dimensional Cu layer structure on top of the Ru surface. Very recent studies in our laboratory (*44*) revealed indeed that higher deposition temperatures support the formation of a homogeneous Cu monolayer and clearly reduce the tendency to form three-dimensional hillocks at this coverage. Since the Cu–Ru bond strength exceeds the sublimation energy of Cu by several kcal/mole it is quite evident why small Cu amounts are spreading on a Ru substrate and form a two-dimensional monolayer before three-dimensional Cu crystallites are growing.

The following paper will demonstrate that close analogies exist between Sinfelt's catalysts and the present model systems with respect to hydrogen chemisorption so that it is believed that the principles of the elementary surface processes can indeed be successfully studied in this way.

ACKNOWLEDGMENTS

The authors are grateful to the Deutsche Forschungsgemeinschaft (SFB 128) for financial support of this work, and to Dr. J. C. Vickerman for a critical reading of the manuscript and for valuable comments. One of us (H.S.) gratefully acknowledges support by the Alexander-von-Humboldt-Stiftung.

REFERENCES

1. See for example: Schwab, G. M., *Disc. Faraday Soc.* **8,** 166 (1950); Dowden, D. A., *J. Chem. Soc.* 242 (1950); Hall, W. K., and Emmett, P. H., *J. Phys. Chem.* **62,** 816 (1958); **63,** 1102 (1959); Sachtler, W. M. H., and van der Plank, P., *Surface Sci.* **18,** 62 (1969); Ponec, V., and Sachtler, and W. M. H., *J. Catal.* **24,** 250 (1972); Ponec, V., *Surface Sci.* **80,** 352 (1979).
2. Sinfelt, J. H., *Acc. Chem. Res.* **10,** 15 (1977).
3. Sinfelt, J. H., *J. Catal.* **29,** 308 (1973).
4. Sinfelt, J. H., *Chem. Eng. News* **50,** 18 (1972).
5. Cecil, R. R., Smak, W. S., Sinfelt, J. H., and Chambers, L. W., *Proc. Div. Refin., Amer. Pet. Inst.* **52,** 203 (1972).
6. Sinfelt, J. H., Lam, Y. L., Cusumano, J. A., and Barnett, A. E., *J. Catal.* **42,** 227 (1976).
7. Prestridge, E. B., Via, G. H., and Sinfelt, J. H., *J. Catal.* **50,** 115 (1977).
8. Helms, C. R., and Sinfelt, J. H., *Surface Sci.* **72,** 229. (1978).
9. Christmann, K., Ertl. G., and Shimizu, H. *Thin Solid Films* **57,** 247 (1979).
10. Christmann, K., and Ertl, G., *Thin Solid Films* **28,** 3 (1975).
11. Conrad, H., Herz, H., and Kuppers, J., *J. Phys. E.* **12,** 369 (1979).
12. Grant, J. T., and Haas, T. W., *Surface Sci.* **21,** 76 (1970).
13. Madey, T. E., Engelhardt, H. A., and Menzel, D., *Surface Sci.* **48,** 304 (1975).
14. Fuggle, J. C., Madey, T. E., Steinkilberg, M., and Menzel, D., *Surface Sci.* **52,** 521 (1975).
15. Madey, T. E., and Menzel, D., *Jpn. J. Appl. Phys.* (Proc. 2nd Intern. Conf. on Solid Surf., Kyoto 1974, Suppl. 2, Part 2, 229).
16. Christmann, K., Schober, O., Ertl, G., and Neumann, M., *J. Chem. Phys.* **60,** 4528 (1974).
17. Behm, R. J., Christmann, K., and Ertl, G., *Solid State Commun.* **25,** 736 (1978).
18. Christmann, K., Ertl, G., and Pignet, T., *Surface Sci.* **54,** 365 (1976).
19. Feulner, P., and Menzel, D., *Verhdlg. DPG* **2,** 559. (1978).
20. Taylor, N. J., *Rev. Sci. Instr.* **40,** 792 (1969).
21. Ertl, G., and Küppers, J., *in* "Low Energy Electrons and Surface Chemistry" p. 7. Verlag Chemie, Weinheim, 1974.
22. Powell, C. J., *Surface Sci.* **44,** 29 (1974).
23. Ponec, V., and Kuijers, F. J., *Surface Sci.* **68,** 294 (1977).
24. Palmberg, P. W., and Rhodin, T. N., *J. Appl. Phys.* **39,** 2425 (1968).
25. King, D. A., *Surface Sci.* **47,** 384 (1975).
26. "Handbook of Chemistry and Physics," 51st ed. The Chemical Rubber Publishing Co., Cleveland, Ohio, 1971.
27. Kraemer, K., and Menzel, D., *Ber. Bunsenges. Phys. Chem.* **78,** 591 (1974).
28. Gartland, P. O., Berge, S., and Slagsvold, B. J., *Phys. Rev. Lett.* **28,** 738 (1972).
29. Ertl, G., and Küppers, J., *in* "Low Energy Electrons and Surface Chemistry" p. 124. Verlag Chemie, Weinheim, 1974.
30. See, for example, the surveys given in: (a) Mais-

sel, L. I., and Glang, R. (Eds.), "Handbook of Thin Film Technology." McGraw Hill, New York, 1970; (b) Hirth, J. P., and Pound, G. M., *in* "Condensation and Evaporation" (B. Chalmer, Ed.). Pergamon Press, Oxford, 1963.

31. Schmidt, L. D., and Gomer, R., *J. Chem. Phys.* **45,** 160 (1966).
32. Polanski, J., and Sidorski, Z., *Surface Sci.* **40,** 282 (1973). Richter, L., and Gomer, R., *Phys. Rev. Lett.* **37,** 763 (1976). Dionne, N., and Rhodin, T. N., *Phys. Rev.* **B 14,** 322 (1976).
33. Newns, D. M., *Phys. Rev.* **178,** 1123 (1969).
34. Jones, J. P., and Roberts, E. W., *Surface Sci.* **69,** 185 (1977).
35. Graham, W. R., and Ehrlich, G., *Phys. Rev. Lett.* **31,** 1407 (1973). Ayrault, G., and Ehrlich, G., *J. Chem. Phys.* **60,** 281 (1974).
36. Knabbe, E. A., and Harsdorff, M., Proc. 4th Intern. Thin Film Congress Loughborough, 1978, in press.
37. Melmed, A. J., *J. Chem. Phys.* **43,** 3057 (1965).
38. Rossini, F. D., "Selected Values of Chemical Thermodynamic Properties," Wagman, D. D., Evans, W. H., Levine, S., and Jaffe, I., 1st ed. U.S. Department of Commerce, 1962.
39. Bauer, E., Poppa, H., Todd, G., and Bonczek, F., *J. Appl. Phys.* **45,** 5164 (1974).
40. Gomer, R., *in* "Field Emission and Field Ionization." Harward University Press, Cambridge, 1966.
41. Smoluchowski, R., *Phys. Rev.* **60,** 661 (1941).
42. Sachtler, W. M. H., *Le Vide* **164,** 67 (1973).
43. Engel, T., and Gomer, R., *J. Chem. Phys.* **52,** 1832 (1970).
44. Vickerman, F. C., Ertl, G., and Christmann, K., in preparation.